Gas-liquid hydrogenation in continuous flow – the effect of mass transfer and residence time in powder packed-bed and catalyst-coated reactors

Nikolay Cherkasov *[a,b], Petr Denissenko [a], Shrirang Deshmukh [a], Evgeny V Rebrov [a,b,c]

[a] School of Engineering, University of Warwick, Coventry CV4 7AL, United Kingdom

[b] Stoli Catalysts Ltd, Coventry, CV3 4DS, UK

[c] Department of Biotechnology and Chemistry, Tver State Technical University, Tver 170026, Russia

corresponding author: n.cherkasov@warwick.ac.uk

Abstract

Catalyst-coated tube reactors have been compared with the reactors packed with catalyst powder in alkyne semi-hydrogenation over a 5 wt.% Pd/ZnO catalyst and cinnamic ester full hydrogenation over a 2.4 wt.% Pd/C catalyst. The “powder packed-bed” reactors (packing with catalyst powder below 30 μm) showed irreproducible performance in time due to mobility of the catalyst layer in the bed which altered the fluidic path and therefore affected the mean liquid residence time and the dispersion. The catalyst-coated tube reactors demonstrated an ideal plug-flow behaviour (Péclet number > 120), while the powder packed-bed showed a considerable back-mixing (Péclet ~ 25). Under all conditions studied, the reaction rate in the powder packed-bed was limited by external mass transfer, while in the coated tube – by the intrinsic kinetics. The coated tubes demonstrated a much lower pressure drop, an improved alkene selectivity, and a 5 times higher throughput compared to the powder packed-bed. The dilution of the catalyst bed with glass beads improved the throughput 4-fold at the expense of 4-fold increase in the pressure drop. In full hydrogenation reaction, the catalyst-coated tube showed a 14 times higher

throughput than in the powder packed-bed at the full alkyne conversion. A reactor model for the catalyst-coated tube has been proposed that takes into account the change in the fluid velocity during the reaction. The model described the reaction kinetics demonstrating that the catalyst-coated tubes can be used as a tool to obtain kinetic data in gas-liquid reactions in flow.

Keywords: hydrogenation; catalyst coating; reactor design; Lindlar; acetylene

1. Introduction

Chemical reactors determine product yield and impose limitations on process conditions, scalability, mass- and heat- transfer rates. Batch reactors are widely used in fine chemicals industry due to high product yield and versatility. Their versatility, however, is counterbalanced by drawbacks of inefficient use of the reactor volume – the batch-wise operation creates many repetitive non-productive operations such as loading or cleaning [1]. Importantly, the mass-transfer rate does not scale-up proportionately to the reactor volume [2–6]. The batch reactors show significant non-uniformities in the liquid velocity during stirring and these non-uniformities (and associated mass-transfer problems) only magnify with the reactor scale [2,4,5].

Continuous flow reactors are increasingly adopted by the industry solving the batch inefficiencies, bringing just-in-time manufacture with low operational costs and improved process safety [1,7,8]. Not surprisingly, all the megaton-scale petrochemical processes are performed in continuous flow for gas-phase and well as gas-liquid heterogeneously-catalysed reactions. The knowledge for such reactor design was accumulating for decades and resulted in a clear understanding of the required dimensions of the catalyst pellets, reactor dimensions, flow rates of gas and liquid to maximise the reaction rates, product selectivity, and catalyst lifetime [9,10].

There are, however, many applications where megaton throughput is undesirable – from catalyst screening and laboratory tests to manufacture of pharmaceuticals and fine chemicals. In these cases, micro-packed-bed reactors with sub-millimitre catalyst particles provide a larger external surface area and decrease inter-pore mass-transfer limitations. The gas-liquid hydrodynamics inside micro-packed-bed filled with the particles 50-500 μm started development relatively recently establishing stability of the start-up procedure [11], pressure drop and liquid hold-up [12], the criteria for radial mass transport and its effect on the reaction rates [13]. In the synthesis of fine chemicals and pharmaceuticals, however, the catalyst particles have to be smaller than 50 μm because the vast majority of commercial catalysts are powders with the particle in the μm range. Such powdered catalysts, such as palladium on charcoal, is difficult to pelletise and pellets are expected to create internal mass-transfer limitations. Creating core-shell catalyst

starting from a given commercial powdered catalyst is also a task of a formidable complexity that goes beyond the focus of the majority chemical manufacturers [14]. Therefore, powdered catalysts are often used in continuous flow hydrogenation [15–18]. Small catalyst dimensions, however, impose limitations on scalability, but increasing catalyst pellet size is undesirable due to pore diffusion limitations.

Structured reactors show a particular promise in improving mass-transfer rates and allowing a more straightforward way for scale-up [19]. The reactors can be numbered up [20,21] or the number of repetitive structural units can be multiplied inside a single reactor. Therefore, it is possible to keep the fluid velocity inside the structural unit constant regardless of the manufacturing scale to ensure predictable behaviour independent of production scale [2,22].

In this work, we aim to compare experimentally the simplest and commercially available packed-bed with structured reactors in terms of mass transfer, residence time distribution, throughput, and selectivity in semi-hydrogenation and full hydrogenation reactions. The packed-bed reactor (referred to as a powder packed-bed thereafter) is a tube filled with a typical hydrogenation catalyst powder with the particle dimensions well below 30 μm; the structured reactor is a tube wall-coated with the same catalyst.

The reactions selected were semi-hydrogenation of 2-methyl-3-butyn-2-ol (MBY) and full hydrogenation of ethyl cinnamate shown in Fig. 1. MBY hydrogenation was selected as an industrially important compound used in vitamin synthesis [23,24]. It is also a representative example for consecutive hydrogenation reactions, where the intermediate (2-methyl-3-buten-2-ol, MBE) is the desired product and full hydrogenation molecule (2-methyl-3-butan-2-ol, MBA) is the major by-product (Fig. 1A). Hydrogenation of ethyl cinnamate (Fig. 1B) is a full hydrogenation example of the compound representative of many fine chemicals with its diverse and bulky functional groups.

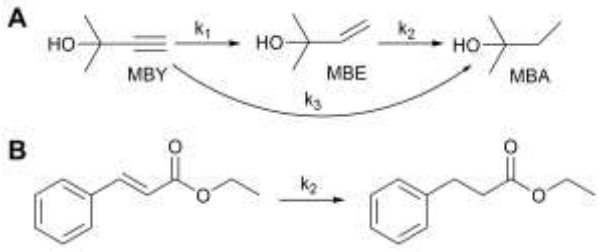

Fig. 1. Schemes of the reactions studied: (A) semi-hydrogenation of 2-methyl-3-butyn-2-ol with 2-methyl-3-buten-2-ol the target product and 2-methyl-3-butanol the main by-product; (B) ethyl cinnamate full hydrogenation.

Alkyne semi-hydrogenation is performed in industry over the Lindlar (Pd doped with Pb supported on $CaCO_3$ and quinoline) [23–25]. The poisons increase alkene selectivity but diminish the reaction rates; Pb from the catalyst can leach and contaminate of the products. Therefore, non-Pb catalysts are gaining popularity with catalysts modified with In, Sn, Bi, Cu, reported to increase alkene selectivity [26–30]. There are also methods to obtain Pd-based catalysts without the second metal applying instead various organic modifies such as thiols, phosphates and others [31–34]. For the first step of the study, we selected a Pd/ZnO catalyst because the catalyst shows high alkene selectivity [35–37], but does not suppress over-hydrogenation. Therefore, all the conclusions can be generalised to a gas-liquid A→B→C reaction. The full hydrogenation reaction was carried out over a 2.4 wt% Pd/C catalyst because the carbon-supported catalysts are the most widely used in hydrogenation reactions. This reaction is representative for typical A→B hydrogenation reaction in fine chemicals industry.

2. Experiment

A 5 wt% Pd/ZnO catalyst (fraction size 1-30 μm, Supplementary SI1) and a tube reactor (316L stainless steel) coated with the same catalyst (coating thickness = 23±3 μm, catalyst loading 100 mg in a 5m tube [36]); a 2.4 wt% Pd/C (fraction size 1-10 μm, Supplementary SI1) and a tube reactor coated with the same catalyst (coating thickness = 21±2.5 μm, catalyst loading 70 mg in a 5m tube [38]) were provided by Stoli Catalysts Ltd and used as received. Isopropanol (98 %), 2-methyl-3-butyn-2-ol (98 %) and ethyl cinnamate (98 %) were purchased from Fischer Scientific.

Previous studies showed excellent catalyst adhesion and achieved remarkable turn-over number (TON) numbers above 1,000,000 [39,40]. The Pd/ZnO catalysts were non-porous with only external area and the BET surface area of 0.5 m^2 g^{-1} [36] while the Pd/C catalysts had the surface area of about 40 m^2 g^{-1}.

Hydrogenation was performed in the bespoke automated continuous flow system described in references [36,41] operated using the OpenFlowChem platform [42,43]. Briefly, a set of mass-flow controllers provided a hydrogen flow (99.9%, BOC) that was combined with a liquid flow from an HPLC pump in a T-mixer. All gas flow rates presented are referred to normal temperature and pressure. A molar ratio between hydrogen and the organic substrate was fixed at 1.05 in all experiments. The reactor, either catalyst-coated tube reactor (1.27 mm ID, 1.60 mm OD) or a packed-bed reactor filled with the catalyst powder (Omnifit column 6.6 mm ID, further details are in Supplementary SI1) was placed in a convection oven and heated to a desired temperature. Forced convection of air provided uniform temperature across the oven with the temperature deviations below 0.1 ^oC measured with a separate thermocouple. The flow entering the reactor flow exchanged heat with the outgoing flow and with the environment (via a heat sink). A back-pressure regulator was used to keep the desired pressure in the reactor. The liquid products were collected into vials for offline analysis with a Shimadzu GC-2010 gas chromatograph equipped with a flame ionisation detector (FID) and a Stabilwax column (10m x 0.15mm x 0.15 μm). Product conversion (*X*) and selectivity (*S*) were calculated with the equations 1-2, where *C* and C^0 are the determined and initial concentrations of the species. In all the cases, the mass balance was better than 99±2% confirming that all the major products were detected.

$$X = 1 - \frac{C_{substrate}}{C^0_{substrate}}, \quad (1)$$

$$S = \frac{C_{product}}{C^0_{substrate} - C_{substrate}}. \quad (2)$$

Fig. 2 shows the setup used for the residence time distribution study. A tracer (0.2-1.0 μL of 0.5 wt% fluorescein in water) was injected (3 mL min^{-1}) with a syringe pump into the gas-liquid

stream before the reactor. Concentration of the dye was determined from the fluorescence signal recorded at the reactor inlet and the outlet with a PointGrey camera at 45 frames per second connected to an Olympus SZX-16 microscope. The optical system of the microscope consisted of an X-cite 120 xenon light source, a blue irradiation light filter, and a yellow receiver light filter to detect primarily the fluorescence signal. The camera was calibrated using a series of standard solutions to show a relative error below 1 %.

The residence time distribution study was carried out in a flow of isopropanol and H_2 to avoid possible reactions with the organic dye. The difference in the fluid density and viscosity between the model and the actual reaction mixture was below 2 %. Hence, the data can be translated to the actual reaction conditions.

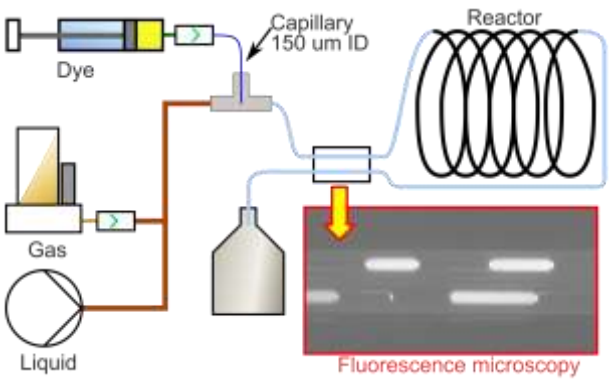

Fig. 2. System for residence time distribution analysis in a gas-liquid flow based on fluorescent microscopy of the inlet and outlet streams.

The concentration profiles of the fluorescent dye obtained at the inlet and the outlet of the reactor were analysed with a procedure described in Supplementary SI2. Briefly, a Fourier deconvolution procedure was performed for the inlet and outlet concentration profiles to account for non-ideal behaviour of the inlet pulse. Equation 3 shows a derivation of the residence time distribution function, where *iFFT* and *FFT* are inverse and forward fast Fourier transform operations, C_{out} and C_{in} are output and input concentration pulses. The pulses were smoothened and normalised prior to computations to reduce noise.

$$RTD(t) = iFFT\left(\frac{FFT(C_{out}(t))}{FFT(C_{in}(t))}\right) . \quad (3)$$

The kinetic modelling of the experimental data had been performed in MATLAB minimising the weighted errors between the experimental and model data by adjusting the variables – the parameters of the model [44].

3. Results and discussion

3.1. Effect of residence time distribution and mass transfer

The presence of mass-transfer limitations was studied in the powder packed-bed and in the catalyst-coated tube reactors – both containing the same 5 wt% Pd/ZnO catalyst in the form of the powder or catalyst coating on the internal walls. The test was performed by changing the catalyst mass and substrate feed rates keeping the weight hourly space velocity (WHSV) constant. In this case, WHSV was calculated with equation 4:

$$WHSV = \frac{Q_{m,MBY}}{m_{cat}}, \quad (4)$$

where $Q_{m,MBY}$ is the mass-flow rate of MBY flowing through the catalyst bed that contains mass of the catalyst m_{cat}. This definition does not include the gas flow rate, but the gas flows selected in the studies were always proportional to the MBY flow rate rendering various reactors with the same WHSV comparable in the sense of having identical inlet flow rates.

The comparison only in terms of WHSV, however, may be misleading. A higher pressure drop in the reactor compresses the hydrogen bubbles (higher contact time) and increases the reaction rate (proportional to hydrogen pressure). Moreover, a high MBY conversion in the reactor results in a substantial gas absorption and a higher contact time that, in turn, further increases conversion.

A more accurate analysis was performed by calculating the apparent reaction rate constant (k_{app}) using equation 5, valid at present experimental conditions as described in the Supplementary SI5.

$$k_{app} = \frac{\Delta C_{MBY}\, Q_L}{(p_{inlet}/2 + p_{outlet}/2)\, n_{Pd}}. \qquad (5)$$

where ΔC_{MBY} is the decrease in MBY concentration in the reactor, Q_L is the liquid flow rate, p is the pressure at the reactor inlet/outlet, and n_{Pd} is the amount of Pd inside the reactor in mol. This formula does not account for various flow behaviour in the reactors, but the values provide an overall comparison for the catalyst throughput in the reactors.

Fig. 3A shows the behaviour of a powder packed-bed reactor at a fixed WHSV but changing catalyst mass. The MBE selectivity fell from 96% to 91% while the MBY conversion increased from 17 to 37% with a higher catalyst loading. The changing conversion indicates the presence of external mass-transfer limitations. MBY conversion also varied from sample to sample under the same conditions likely due to liquid channelling or variable catalyst wetting [45]. The apparent reaction rate takes into account the pressure drop in the reactor by using a known proportionality between pressure and the hydrogenation reaction rate [22,36,46,47]. The apparent rate constant (Fig. 3A) decreased with the catalyst loading. In general, the reaction rates should be constant if no external mass-transfer limitations are observed or increase in case of external mass-transfer limitations. The studied system, however, showed an inverse behaviour which indicates the effect of gas-liquid hydrodynamics on the flow rates. The experiments performed and at the outlet pressure of 5 bar and under the same liquid flow rates (but different catalyst masses) shows the same overall trends (in Supplementary SI2).

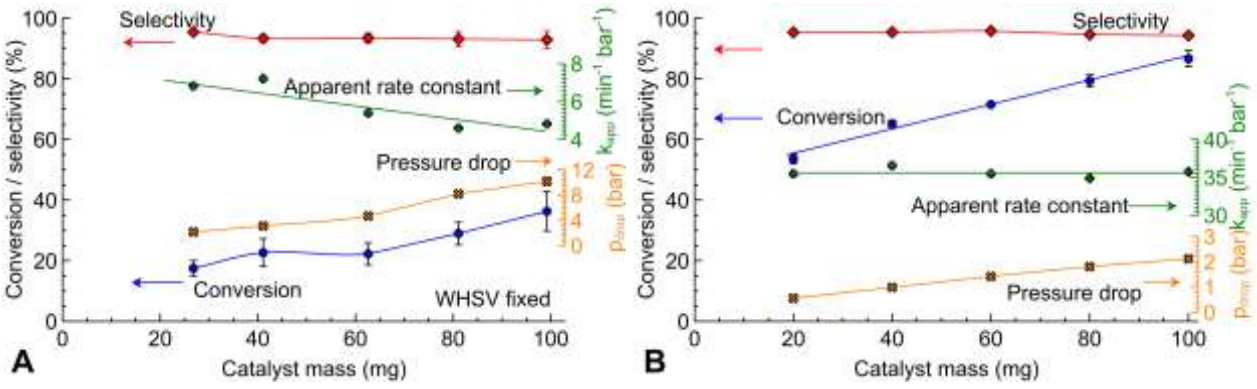

Fig. 3. Effect of the catalyst loading on the pressure drop, MBY conversion, and MBE selectivity over a 5 wt% Pd/ZnO catalyst in (A) powder packed-bed, and (B) catalyst-coated tube reactors.

Reaction conditions: 400 mM MBY solution in IPA, H_2/MBY initial molar ratio 1.05, WHSV 0.9 $g_{MBY}\ g_{cat}^{-1}\ min^{-1}$, temperature 50 ^oC, outlet pressure 1 bar.

Fig. 3B shows the performance of the catalyst-coated tube reactor under the same conditions. The MBY conversion was notably higher, while the MBE selectivity was constant. The increasing catalyst mass in the tube reactor resulted in a higher MBY conversion. The apparent reaction rate, however, was stable confirming the absence of mass-transfer limitations. This is not surprising considering quick mass-transfer rates and micromixing observed in Taylor flow inside the mm-range tubes [48–50]. The apparent reaction rate was also a factor of 5 higher in the tube reactor compared to the powder packed-bed showing limited catalyst utilisation in the powder packed-bed likely due to external mass-transfer limitations.

Compared to the powder packed-bed, the tube reactors (Fig. 3) also showed two notable features: (i) stable MBY conversion over time, and (ii) a substantially lower pressure drop. The consistent conversion demonstrates excellent control of hydrodynamics in the tube reactor. The difference in the pressure drop is particularly remarkable considering that the powder packed-bed reactor was 20 mm long, while the tube reactor was 4.5 m long. The difference in the pressure drop is not surprising because the pressure drop through a channel is inversely proportional to the opening diameter in the power of 4. In the powder packed-bed reactor, most of the flow channelled through the openings created by larger particles while smaller particles had no or little flow around them “eliminating” them from the reaction and explaining such a low apparent reaction rate.

Fig. 4A shows representative residence time distribution profiles for both reactors.

The powder packed-bed reactor demonstrated a broad and asymmetrical residence time distribution. The broadening was created by non-uniform liquid velocities [5]. The tube reactor showed, unsurprisingly, the narrowest distribution because the liquid slugs were separated by the slugs of gas reducing back-mixing in the Taylor flow. Some dispersion observed was caused by

the liquid film around the gas slugs which resulted in the exchange of liquid between the liquid slugs [15,51–53].

The powder packed-bed reactors diluted with the glass beads are widely used to increase the reactor performance [54,55]. Hence, we diluted the Pd/ZnO catalyst particles (1-10 μm) with glass beads (210-290 μm, Supplementary SI1) and studied in hydrogenation. Although Herk et al. [45] recommended diluting the catalyst particles with inert material of the same dimensions to avoid channelling, this approach is impractical for fine catalyst particles because it would result in a prohibitively high pressure drop. The residence time distribution obtained for the diluted powder packed-bed was narrower indicating lower liquid channelling compared to the reactor packed only with the catalyst powder.

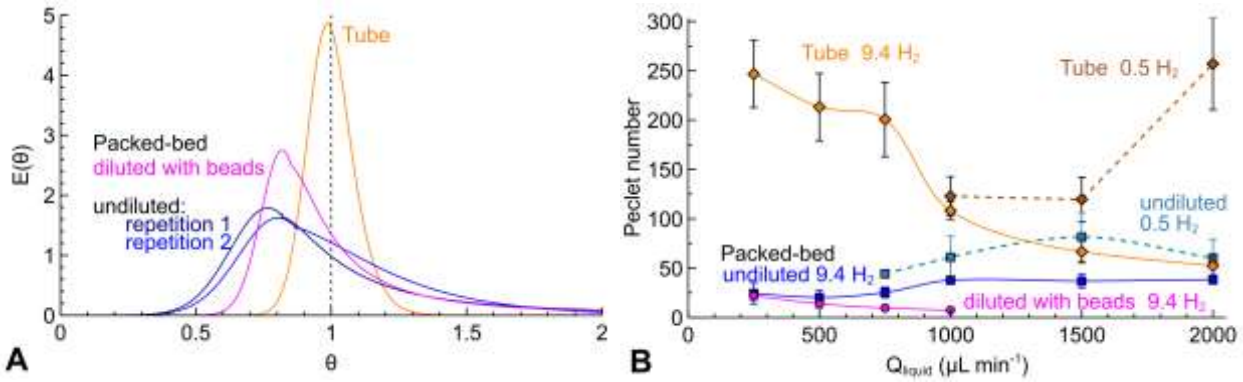

Fig. 4. (A) Representative residence time distribution obtained in a tube and packed-bed reactors filled with the Pd/ZnO powder (alone or diluted with glass beads). Isopropanol flow of 250 μL min^{-1}, 2.3 mL min^{-1} H_2. (B) Effect of the liquid flow rate on the Péclet number obtained in the tube and packed-bed reactors. Gas flow rate increased proportionally to the liquid flow at 9.4 mL_{gas} mL_{liq}^{-1} (solid lines) or 0.5 mL_{gas} mL_{liq}^{-1} (dashed lines).

The two reactors were also compared in terms of dimensionless axial dispersion expressed in the form of the Péclet number (*Pe*) calculated by solving equation 6 [56],

$$\frac{\sigma^2}{t_m^2} = \frac{2}{Pe} - \frac{2}{Pe^2}(1 - e^{-Pe}), \qquad (6)$$

where t_m is the average residence time and σ is the dispersion of the residence time distribution obtained from the pulse experiments (Fig. 4). The Péclet number characterises the ratio of convective and diffusive mass-transfer rates. The values above 100 indicate a plug-flow behaviour of a reactor with excellent control over the residence time. Low Péclet number shows high dispersion that decreases the MBE selectivity because the highest MBE yield can be observed only at certain residence times over a Pd/ZnO catalyst [36,57,58].

The tube reactor showed high Péclet numbers under a wide range of flow rates (Fig. 4B). Only at the liquid flow rate above 1 mL min^{-1}, the dispersion became significant because a huge H_2 excess formed a slug-annular flow regime with a continuous liquid film along the tube reactor. The reactions in slug-annular flow have little relevance under the reaction conditions because H_2 consumption during the reaction results in the domination of the Taylor flow regime [27]. This Taylor flow behaviour was simulated by feeding comparable amounts of gas and liquid into the reactor making the tube behave as an ideal plug-flow reactor with the Péclet numbers above 125.

On the contrary, the powder packed-bed reactor showed rather low Péclet numbers (Fig. 4B). At the liquid flow rates below 500 µL min^{-1}, the reactors diluted with glass beads and filled only with the Pd/ZnO catalyst behaved similarly. The increasing flow rate, however, resulted in the decreasing Péclet number for the diluted reactor, while the undiluted reactor showed constant Péclet numbers – the values that are still short of the plug-flow behaviour. High dispersion observed in the diluted powder packed-bed reactor was expected considering large internal volume where liquid back-mixing can take place.

Therefore, the reactors packed with a powdered catalyst showed considerable mass-transfer limitations in addition to high axial dispersion. Importantly, the reactors showed irreproducible behaviour caused by altering the fluidic path. The tube reactors wall-coated with the catalyst showed essentially a plug-flow behaviour with a narrow residence time distribution and no external mass-transfer limitations.

3.2. Alkyne semi-hydrogenation

Fig. 5A shows the effect of the liquid and gas flow rates on the performance of the powder packed-bed reactor in selective hydrogenation over a Pd/ZnO catalyst at an H_2 to substrate molar ratio of 1.05. Increasing liquid flow rate resulted in a lower MBY conversion due to (i) higher amount of substrate and (ii) a shorter residence time [36].

Fig. 5B and C show that pressure and temperature resulted in a higher MBY conversion but lower MBE selectivity. The conversion decreased at the temperature of 75 ^{o}C likely because of increasing vapour pressure of isopropanol and a corresponding decrease in the hydrogen vapour pressure. The MBE selectivity was in the range of 87-92% which is below the typical selectivity of 95% observed over the Pd/ZnO catalysts at low MBY conversion [36,57,58].

Wide confidence intervals in MBY conversion (Fig. 5) are another notable feature in the powder packed-bed hydrogenation. These intervals are obtained by collecting 5-7 consecutive liquid samples– the samples that already significantly averaged the reactor performance over 3-140 s to collect a sample depending on the liquid flow rate. Therefore, liquid channelling in the powder packed-bed reactors significantly limits selectivity and conversion rendering them to be unstable in time.

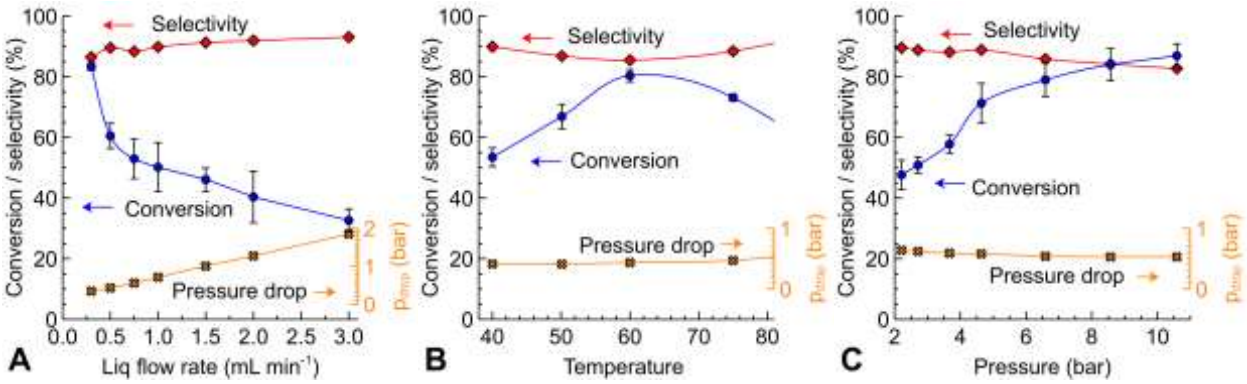

Fig. 5. Effect of (A) flow rate, (B) temperature, and (C) pressure on MBY conversion, MBE selectivity, and pressure drop in a 6.6 mm reactor packed with 100 mg of a 5 wt% Pd/ZnO catalyst powder. Reaction conditions: 400 mM MBY solution in IPA, H_2/MBY initial molar ratio 1.05, ambient outlet pressure, (A) 50 ^{o}C; (B) 0.5 mL min^{-1} liquid flow or (C) 2 mL min^{-1} liquid flow.

Fig. 6 shows the data for the powder packed-bed reactors studied at the back-pressure of 5 bar. A higher reaction pressure results in faster intrinsic reaction rates and more severe mass-transfer limitations evidenced by the virtual independence of MBY conversion on the reaction pressure and temperature. The powder packed-bed reactor diluted with glass beads (Fig. 6D) – a widely used practice in organic chemistry – shows a 1.5 – 4 higher compared to the undiluted packed-bed under the same experimental conditions (Fig. 6A). The conversion reached a maximum of 90% at WHSV 0.35 min^{-1}. The selectivity monotonously increased with WHSV from 70% to 88% - a remarkably low value considering that it should have been at least 95% based on the data obtained in the gradientless batch reactors [57–62].

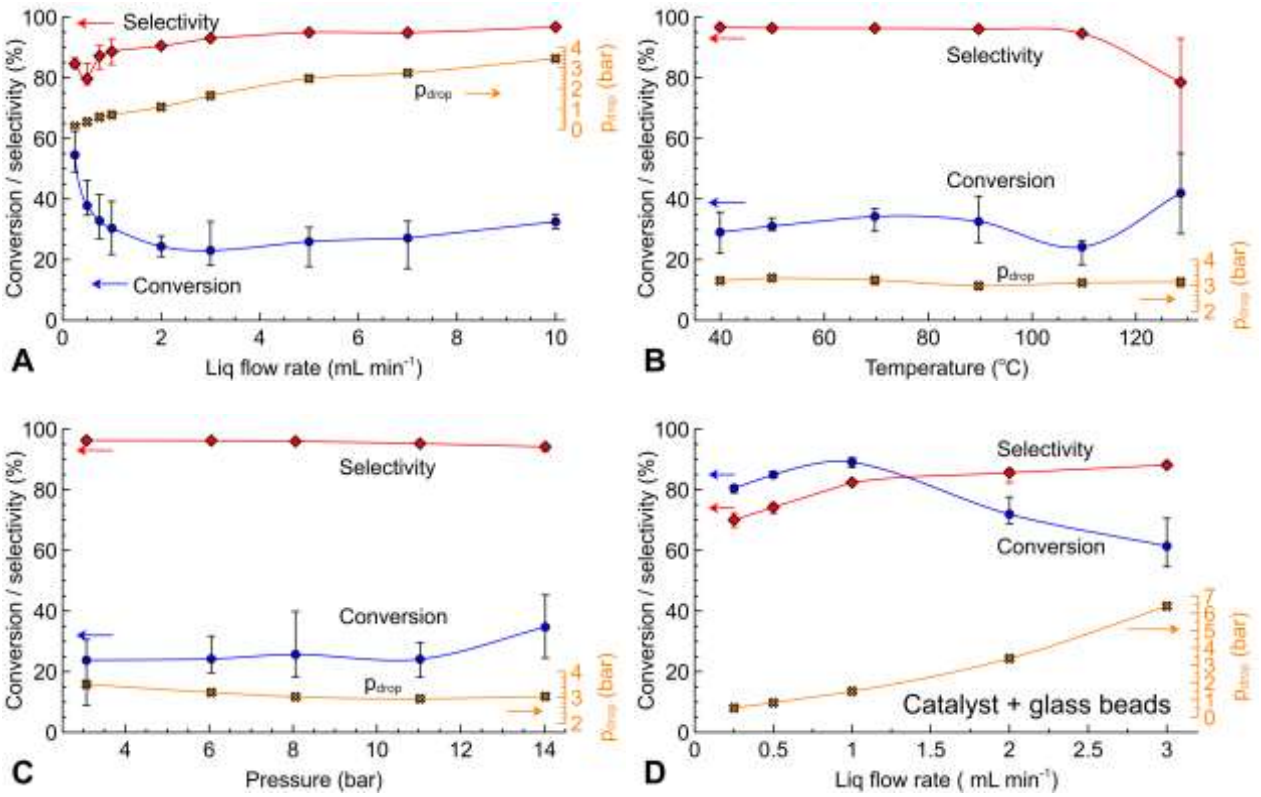

Fig. 6. Effect of (A) flow rate, (B) temperature, and (C) pressure on MBY conversion, MBE selectivity, and pressure drop in a 6.6 mm reactor packed with 100 mg of a 5 wt% Pd/ZnO catalyst powder. Reaction conditions: 400 mM MBY solution in IPA, H_2/MBY initial molar ratio 1.05, (A) 50 °C, 5 bar; (B) 10 mL min^{-1} liquid flow, 5 bar; (C) 50 °C, 10 mL min^{-1} liquid flow. (D)

The same experiment in the reactor filled with 100 mg of a 5 wt% Pd/ZnO catalyst powder diluted with 2 g glass beads.

The diluted powder packed-bed reactor, compared to the undiluted reactor, showed a substantially higher pressure drop. The glass beads formed wide intra-particle voids and should create a negligible pressure drop on their own. A substantially higher pressure drop, therefore, was created by with the smaller catalyst particles blocking the gaps in between the glass beads. Hence, the diluted reactor creates a pressure drop substantially higher than the undiluted powder packed-bed reactor.

The experiments were performed in the catalyst-coated tube reactor containing the same Pd/ZnO catalyst, Fig. 7. In these experiments, the catalyst loading was decreased 5-fold compared to the powder packed-bed to slow down the reaction. A much lower catalyst loading demonstrates a dramatically higher performance of the catalyst-coated tube reactors compared to the powder packed-bed (Fig. 3).Under such conditions, the void reactor volumes became comparable – 0.8 mL for the powder packed-bed and 1.2 mL for the catalyst-coated tube.

Increasing the liquid flow rates (Fig. 7A) resulted, as expected, in decreasing MBY conversion and increasing MBE selectivity. However, the conversion fell when the liquid flow rate decreased from 1.5 min^{-1} to 1.0 min^{-1} likely because a full H_2 consumption was observed and the two-phase fluid velocity decreased resulting in insufficient mass transfer caused by the liquid recirculation inside the slugs. The conversion first increased and then decreased with temperature (Fig. 7B). A decrease in conversion at 75 ^oC was because the proximity to the solvent boiling point resulted in decreasing the H_2 partial pressure in the reactor [46]. Higher pressure also had a predictable effect of increasing conversion up to 3 bar (Fig. 7C). A further increase in pressure resulted in the conversion decline likely because of the same mass-transfer limitations observed in the slow-moving gas-liquid stream. It is worth noting, that when complete H_2 consumption was avoided, the highest yield of 86.5% was observed. The activation energy (accounting for the solvent vapour pressure, Supplementary SI3) was 24.3 kJ mol^{-1} – in good agreement with the literature

data of 25.2 kJ mol^{-1} [63] and 28.4 kJ mol^{-1} [36] indicating that the reaction rates were limited by intrinsic kinetics.

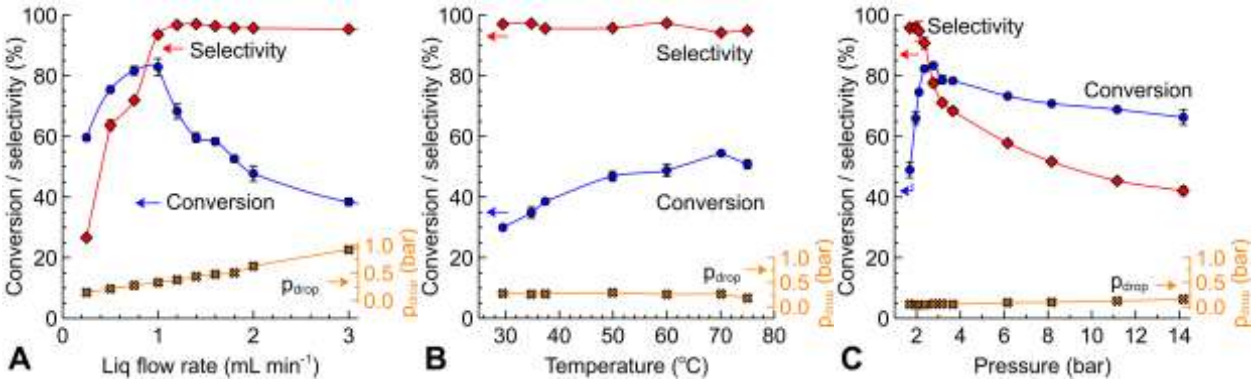

Fig. 7. Effect of (A) flow rate, (B) temperature, and (C) pressure on MBY conversion, MBE selectivity and pressure drop in a 1 m catalyst-coated tube reactor wall-coated with 20 mg 5 wt% Pd/ZnO catalyst. Reaction conditions: 400 mM MBY solution in IPA, H_2/MBY initial molar ratio 1.05, (A) 50 °C, 1 bar; (B) 2 mL min^{-1} liquid flow, 1 bar; (C) 50 °C, 2 mL min^{-1} liquid flow.

Thus, the powder packed-bed reactors show a rather poor performance in gas-liquid reactions. Dilution of the catalyst powder with the larger particles such as glass beads increases conversion and selectivity, but creates an additional pressure loss (energy consumption). Moreover, the selectivity towards an intermediate product remains low. These problems may be circumvented in a recycle mode [64] but it requires much higher flow rates and eliminates the advantages of high space-time yield of continuous systems converting them, in effect, into a tank stirred by the reactant flow. The catalyst-coated tube reactor, on the contrary, showed a considerably higher conversion and selectivity at a low pressure drop in a single-pass operation.

3.3. Alkene full hydrogenation

The powder packed-bed reactors showed low selectivity towards the intermediate product of semi-hydrogenation. At the next step, we studied a full hydrogenation reaction. Full hydrogenation reactions are widely used in industry and may represent semi-hydrogenation if the optimised catalyst provides no or little over-reaction.

Fig. 8 shows the results of ethyl cinnamate hydrogenation in the powder packed-bed and catalyst-coated tube reactors operating at a similar conversion. Both reactors can reach a full ethyl cinnamate conversion with undetectable by-product formation. The performance, however, is remarkably different. The increasing liquid flow rate resulted in a falling conversion, as expected, in both reactors (Fig. 8A, D). However, the liquid flow rate required for the same conversion of 80% (other parameters being equal) was dramatically different – the powder packed-bed reactor required a factor of 14 lower feed rate. The reaction temperature (Fig. 8B, E) and pressure (Fig. 8C, F) had a similar effect. The activation energy observed is 42 kJ mol^{-1}. Hence, the powder packed-bed reactors show a significantly lower catalyst utilisation and high pressure drop compared to the catalyst-coated tube reactors.

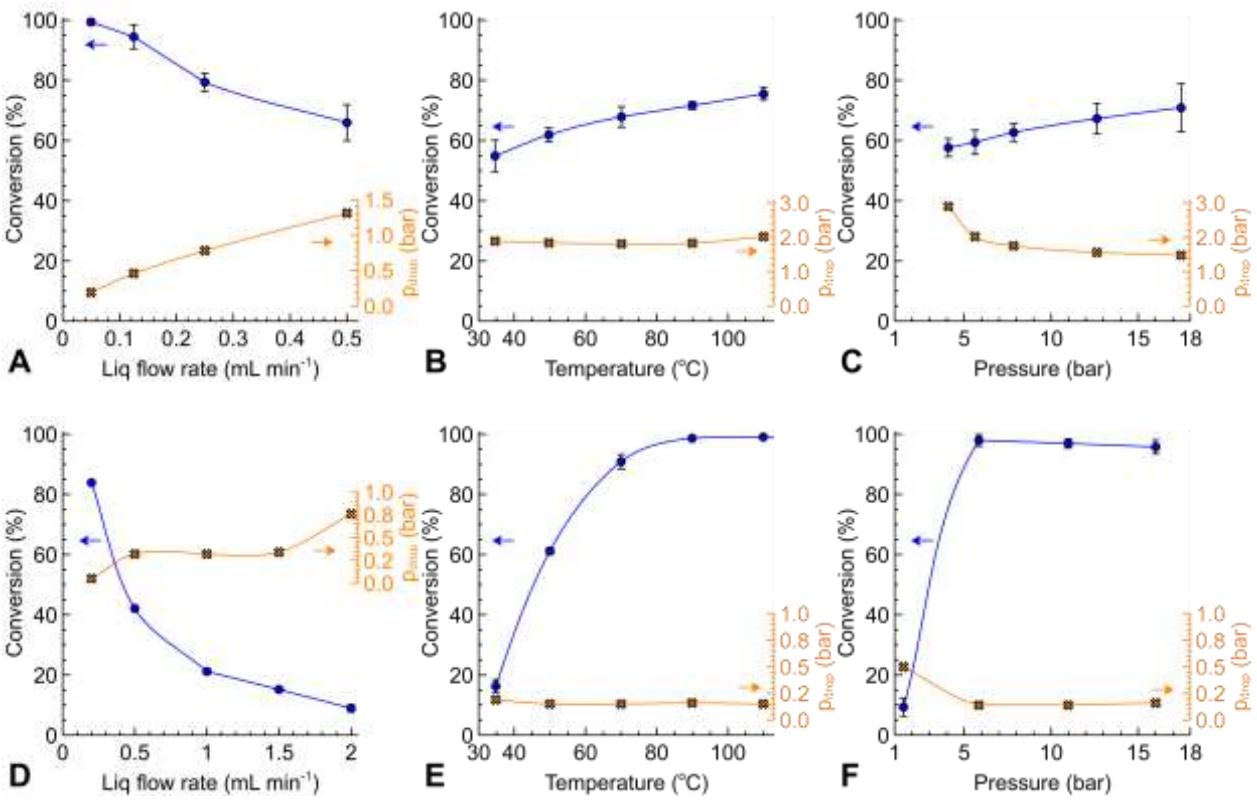

Fig. 8. Effect of (A, D) flow rate, (B, E) temperature, and (C, F) pressure on ethyl cinnamate conversion and pressure drop in either (A, B, C) a 6.6 mm reactor packed with 360 mg of a 2.4 wt% Pd/C catalyst powder or (D, E, F) 1 m catalyst-coated tube reactor wall-coated with the 15 mg of the same catalyst. Reaction conditions: 400 mM substrate in acetone, 5% stoichiometric

excess of H_2, (A, D) 50 °C, 5 bar; (B) WHSV 0.09 g_{MBY} g_{cat}^{-1} min^{-1}, 5 bar; (C) 50 °C, WHSV 0.09 g_{MBY} g_{cat}^{-1} min^{-1}; (D) WHSV 5.0 g_{MBY} g_{cat}^{-1} min^{-1}, 5 bar; (E) 50 °C, WHSV 5.0 g_{MBY} g_{cat}^{-1} min^{-1}.

3.4. Reactor model

A model was proposed to obtain quantitative insights into the reaction kinetics. The model combines the reaction kinetics with the convection flow in the reactor and accounts for decreasing fluid velocity caused by hydrogen consumption. Considering that the Péclet number was above 100, the reactor was modelled an ideal plug-flow reactor. The liquid residence time was calculated with equation 7, where $V_{reactor}$ is the volume of the reactor filled with the catalyst, Q is the volumetric flow rate of liquid and gas at the inlet and outlet of the reactor. Derivation of the model (provided in Supplementary SI3) shows that the model is applicable for the gas-liquid reactor with uniform catalyst distribution along the length, operated in a slug flow regime at a constant hydrogen consumption rate (zero order in respect to substrate is observed for most hydrogenation reactions [36,57,65]) and a negligible pressure drop.

$$t_{res} = \frac{V_{reactor}}{Q_L + \frac{1}{2}(Q_{gas,in} + Q_{gas,out})}. \quad (7)$$

The MBY semi-hydrogenation was described with a Langmuir-Hinshelwood kinetics considering 3 reaction stages of hydrogenation: MBY to MBE (rate is r_1), MBE to MBA (r_2), and a direct MBY to MBA (r_3), Fig. 1. The change in the reactant concentrations is presented in equations 8 – 10, where V_L is the volume of liquid in the reactor, m_{cat} is the catalyst mass, ω_{cat} is the mass fraction of Pd with the molar mass of M_{Pd}.

$$\frac{dC_{MBY}}{dt} = \frac{m_{cat}\,\omega_{Pd}}{V_L\,M_{Pd}}\,(-r_1 - r_3), \quad (8)$$

$$\frac{dC_{MBE}}{dt} = \frac{m_{cat}\,\omega_{Pd}}{V_L\,M_{Pd}}\,(r_1 - r_2), \quad (9)$$

$$\frac{dC_{MBA}}{dt} = \frac{m_{cat}\,\omega_{Pd}}{V_L\,M_{Pd}}\,(r_2 + r_3). \quad (10)$$

The individual reaction rates (equations 11 – 13) were modelled following the approach of Duca et al. [65] considering strong adsorption of MBY, and adsorption of MBE with the adsorption constants of Q_{MBE} ($Q_{MBE} = K_{MBE} / K_{MBY}$). The full hydrogenation of cinnamic ether was modelled using the same system considering the same model, but using only the MBE to MBA hydrogenation step.

$$r_1 = k_1 \frac{c_{MBY}\, p_{H2}}{c_{MBY} + Q_{MBE}\, c_{MBE}}, \qquad (11)$$

$$r_2 = k_2 \frac{Q_{MBE}\, c_{MBE}\, p_{H2}}{c_{MBY} + Q_{MBE}\, c_{MBE}}, \qquad (12)$$

$$r_3 = k_3 \frac{c_{MBY}\, p_{H2}}{c_{MBY} + Q_{MBE}\, c_{MBE}}. \qquad (13)$$

Fig. 9 shows the comparison of the experimental and modelled concentration of the reaction species, which are in excellent agreement for both MBY and ethyl cinnamate hydrogenation studied. The details on the fitting as well as the tables with the data are presented in Supplementary SI6.

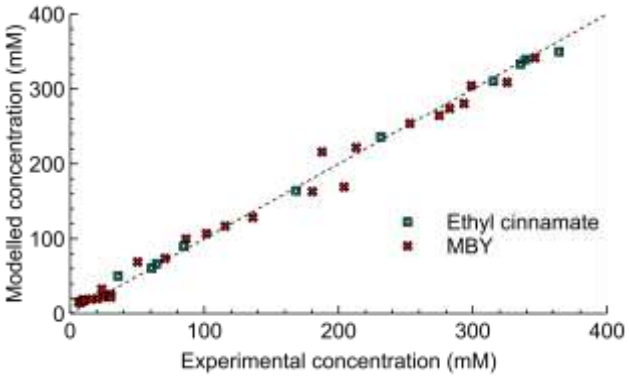

Fig. 9. Comparison of the experimental and modelled concentrations of species for MBY ethyl cinnamate hydrogenation.

The apparent kinetic parameters obtained are listed in Table 1. Considering the average size of Pd nanoparticles in the Pd/ZnO catalyst of 4.2 nm [36], the MBY turn-over frequency (TOF) at the ambient pressure is 0.9 s^{-1} at 50 ^{o}C. Some literature reported the TOF values of MBY semi-hydrogenation an order of ~10 s^{-1} over Pd/ZnO catalysts [57,58,66], while the other reports [32,62,67] were in line with the TOF values observed in the present study. Hence, the catalyst

activity depends on the preparation method and is in line with the literature. The Pd/C catalyst used for ethyl cinnamate hydrogenation had the Pd particle size of 4.0 nm [38] which corresponds to a TOF of 0.6 s^{-1}, in line with a literature value of 0.3 s^{-1} [68].

Table 1. Apparent rate and relative adsorption constants obtained for MBY and ethyl cinnamate hydrogenation in the tube reactors.

	MBY	Ethyl cinnamate
k_1 (bar^{-1} h^{-1})	1404	–
k_2 (bar^{-1} h^{-1})	537	356
k_3 (bar^{-1} h^{-1})	93	–
Q_{alkene}	0.013	–

Thus, the catalyst-coated tube reactors can be employed to analyse fast reaction kinetics. The possibility for quick screening of the reaction conditions without the need to re-start batch experiments as well as the absence of mass-transfer limitations are important factors in simplification and acceleration of the kinetic analysis.

4. Conclusions

We have experimentally compared the performance of catalyst-coated tube reactors and reactors packed with the catalyst powders widely used in the laboratory-scale synthesis of fine chemicals. The catalyst-coated tube reactors showed superior performance – the absence of external mass-transfer limitations on the hydrogenation reaction rates, narrow and tightly reproducible residence time distribution.

The two model reactions studied – alkyne semi-hydrogenation over a Pd/ZnO catalyst demonstrated a dramatic difference between the two reactors. It was impossible to obtain a high yield of the intermediate alkene in the powder packed-bed reactor due to over-hydrogenation into

alkane; moreover, the reactor performance was not reproducible because the main fluidic path continuously changed due to mobility of the catalyst powder. The catalyst-coated tube reactor under the same conditions showed the reaction rates 5 times higher. Moreover, the narrow residence time distribution in the coated tubes resulted in excellent alkene selectivity. The full hydrogenation of ethyl cinnamate, which has no substantial side-reactions, could be carried out at full conversion in both reactors studied over the Pd/C catalyst. However, the coated reactor showed the throughput 14 times higher compared to the reactor packed with the same catalyst due to the absence of external mass-transfer limitations.

The dramatic decrease in the reaction rates and selectivity observed in the powder packed-bed reactors compared to catalyst-coated tubes shows the importance of proper reactor design. In case of the packed-bed reactors, the catalyst particles shall be above 40 μm and have tightly controlled particle size distribution. Packing of the reactor with the catalyst powder designed for stirred tanks is not the shortcut, and even not the way for continuous flow hydrogenation even at a relatively small 0.1-1 kg per day synthesis scale.

The reactor model had been developed for the catalyst-coated tube reactors. The model takes into account consumption of hydrogen inside the reactor and allows for analysis of the reaction kinetics in a continuous flow, much faster compared to large-scale batch experiments that require laborious repetition.

Acknowledgement

The authors are grateful to InnovateUK (grant # 900041) for the support of the work. NC acknowledges support from IchemE Andrew Fellowship.

Conflict of interest

NC and EVR are founders and directors of Stoli Catalysts Ltd.

References

[1] D.M. Roberge, L. Ducry, N. Bieler, P. Cretton, B. Zimmermann, Microreactor Technology:

A Revolution for the Fine Chemical and Pharmaceutical Industries?, Chem. Eng. Technol. 28 (2005) 318–323. doi:10.1002/ceat.200407128.

[2] E.H. Stitt, Alternative multiphase reactors for fine chemicals: A world beyond stirred tanks?, Chem. Eng. J. 90 (2002) 47–60. doi:10.1016/S1385-8947(02)00067-0.

[3] B.H. Stitt, M. Marigo, S. Wilkinson, T. Dixon, How Good is Your Model ?, Johnson Matthey Technol. Rev. 59 (2015) 74–89. doi:10.1595/205651315X686804 JOHNSON.

[4] A.R. Rammohan, A. Kemoun, M.H. Al-Dahhan, M.P. Dudukovic, A lagrangian description of flows in stirred tanks via computer-automated radioactive particle tracking (CARPT), Chem. Eng. Sci. 56 (2001) 2629–2639. doi:10.1016/S0009-2509(00)00537-6.

[5] M.H. Sankey, D.J. Holland, A.J. Sederman, L.F. Gladden, Magnetic resonance velocity imaging of liquid and gas two-phase flow in packed beds, J. Magn. Reson. 196 (2009) 142–148. doi:10.1016/j.jmr.2008.10.021.

[6] J. Hajek, D.Y. Murzin, Liquid-Phase Hydrogenation of Cinnamaldehyde over a Ru - Sn Sol - Gel Catalyst . 1 . Evaluation of Mass Transfer via a Combined Experimental / Theoretical Approach, Ind. Eng. Chem. Res. 43 (2004) 2030–2038. doi:10.1021/ie0340802.

[7] K.F. Jensen, Microreaction engineering — is small better?, Chem. Eng. Sci. 56 (2001) 293–303. doi:10.1016/S0009-2509(00)00230-X.

[8] K.F. Jensen, Flow Chemistry—Microreaction Technology Comes of Age, AlChe. 63 (2017) 858–869. doi:10.1002/aic.15642.

[9] S.T. Sie, R. Krishna, Process Development and Scale Up: III. Scale-up and scale-down of trickle bed processes, Rev. Chem. Eng. 14 (1998) 203–252. doi:10.1515/REVCE.1998.14.3.203.

[10] D.E. Mears, The role of axial dispersion in trickle-flow laboratory reactors, Chem. Eng. Sci. 26 (1971) 1361–1366. doi:10.1016/0009-2509(71)80056-8.

[11] N. Márquez, P. Castaño, J.A. Moulijn, M. Makkee, M.T. Kreutzer, Transient behavior and

stability in miniaturized multiphase packed bed reactors, Ind. Eng. Chem. Res. 49 (2010) 1033–1040. doi:10.1021/ie900694r.

[12] J. Zhang, A.R. Teixeira, L.T. Kogl, L. Yang, K.F. Jensen, Hydrodynamics of Gas–Liquid Flow in Micropacked Beds: Pressure Drop, Liquid Holdup, and Two-Phase Model, AIChE J. 63 (2017) 4694–4704. doi:10.1002/aic.15807.

[13] J.A. Moulijn, M. Makkee, R.J. Berger, Catalyst testing in multiphase micro-packed-bed reactors; criterion for radial mass transport, Catal. Today. 259 (2016) 354–359. doi:10.1016/j.cattod.2015.05.025.

[14] Y. Liu, N. Cherkasov, P. Gao, J. Fernández, M.R. Lees, E. V Rebrov, The enhancement of direct amide synthesis reaction rate over TiO2@SiO2@NiFe2O4 magnetic catalysts in the continuous flow under radiofrequency heating, J. Catal. 355 (2017) 120–130. doi:10.1016/j.jcat.2017.09.010.

[15] A. Tanimu, S. Jaenicke, K. Alhooshani, Heterogeneous catalysis in continuous flow microreactors: A review of methods and applications, Chem. Eng. J. 327 (2017) 792–821. doi:10.1016/j.cej.2017.06.161.

[16] L.J. Durndell, K. Wilson, A.F. Lee, Platinum-catalysed cinnamaldehyde hydrogenation in continuous flow, RSC Adv. 5 (2015) 80022–80026. doi:10.1039/C5RA14984C.

[17] C. Moreno-Marrodan, F. Liguori, P. Barbaro, Continuous-flow processes for the catalytic partial hydrogenation reaction of alkynes, Beilstein J. Org. Chem. 13 (2017) 734–754. doi:10.3762/bjoc.13.73.

[18] S.H. Lau, A. Galván, R.R. Merchant, C. Battilocchio, J.A. Souto, M.B. Berry, S. V. Ley, Machines vs Malaria: A Flow-Based Preparation of the Drug Candidate OZ439, Org. Lett. 17 (2015) 3218–3221. doi:10.1021/acs.orglett.5b01307.

[19] M.T. Kreutzer, F. Kapteijn, J.A. Moulijn, Shouldn’t catalysts shape up? Structured reactors in general and gas-liquid monolith reactors in particular, Catal. Today. 111 (2006) 111–118. doi:10.1016/j.cattod.2005.10.014.

[20] M. Al-Rawashdeh, L.J.M. Fluitsma, T.A. Nijhuis, E. V. Rebrov, V. Hessel, J.C. Schouten, Design criteria for a barrier-based gas-liquid flow distributor for parallel microchannels, Chem. Eng. J. 181–182 (2012) 549–556. doi:10.1016/j.cej.2011.11.086.

[21] M. Al-Rawashdeh, F. Yue, N.G. Patil, T.A. Nijhuis, V. Hessel, J.C. Schouten, E. V. Rebrov, Designing flow and temperature uniformities in parallel microchannels reactor, AIChE J. 60 (2014) 1941–1952. doi:10.1002/aic.14443.

[22] Y. Elias, P. Rudolf von Rohr, W. Bonrath, J. Medlock, A. Buss, A porous structured reactor for hydrogenation reactions, Chem. Eng. Process. Process Intensif. 95 (2015) 175–185. doi:10.1016/j.cep.2015.05.012.

[23] W. Bonrath, J. Medlock, J. Schutz, B. Wustenberg, T. Netscher, B. Wüstenberg, T. Netscher, Hydrogenation in the Vitamins and Fine Chemicals Industry – An Overview, In: I. Karame (Ed.) Hydrogenation, InTech, Rijeka, 2012, pp. 69-90., InTech, 2012. doi:10.5772/3208.

[24] M. Eggersdorfer, D. Laudert, U. Létinois, T. McClymont, J. Medlock, T. Netscher, W. Bonrath, One hundred years of vitamins-a success story of the natural sciences, Angew. Chemie Int. Ed. 51 (2012) 12960–12990. doi:10.1002/anie.201205886.

[25] B. Tripathi, L. Paniwnyk, N. Cherkasov, A.O. Ibhadon, T. Lana-Villarreal, R. Gómez, Ultrasound-assisted selective hydrogenation of C-5 acetylene alcohols with Lindlar catalysts, Ultrason. Sonochem. 26 (2015) 445–451. doi:10.1016/j.ultsonch.2015.03.006.

[26] J.A. Anderson, J. Mellor, R.K.P.K. Wells, Pd catalysed hexyne hydrogenation modified by Bi and by Pb, J. Catal. 261 (2009) 208–216. doi:10.1016/j.jcat.2008.11.023.

[27] N. Cherkasov, A.O. Ibhadon, E. V. Rebrov, Solvent-free Semihydrogenation of Acetylene Alcohols in a Capillary Reactor coated with a Pd-Bi/TiO2 Catalyst, Appl. Catal. A Gen. 515 (2016) 108–115. doi:10.1016/j.apcata.2016.01.019.

[28] S.K. Johnston, N. Cherkasov, E. Pérez-Barrado, A. Aho, D.Y. Murzin, A.O. Ibhadon, M.G. Francesconi, Pd 3 Sn nanoparticles on TiO 2 and ZnO supports as catalysts for semi-

hydrogenation: Synthesis and catalytic performance, Appl. Catal. A Gen. 544 (2017) 40–45. doi:10.1016/j.apcata.2017.07.005.

[29] N. López, C. Vargas-Fuentes, Promoters in the hydrogenation of alkynes in mixtures: insights from density functional theory, Chem. Commun. 48 (2012) 1379–1391. doi:10.1039/c1cc14922a.

[30] T.A. Nijhuis, G. van Koten, J.A. Moulijn, Optimized palladium catalyst systems for the selective liquid-phase hydrogenation of functionalyzed alkynes, Appl. Catal. A Gen. 238 (2003) 259–271. doi:10.1016/S0926-860X(02)00372-1.

[31] P.T. Witte, P.H. Berben, S. Boland, E.H. Boymans, D. Vogt, J.W. Geus, J.G. Donkervoort, BASF NanoSelect™ technology: Innovative supported Pd- and Pt-based catalysts for selective hydrogenation reactions, Top. Catal. 55 (2012) 505–511. doi:10.1007/s11244-012-9818-y.

[32] Z. Wu, N. Cherkasov, G. Cravotto, E. Borretto, A.O. Ibhadon, J. Medlock, W. Bonrath, Ultrasound- and Microwave-Assisted Preparation of Lead-Free Palladium Catalysts: Effects on the Kinetics of Diphenylacetylene Semi-Hydrogenation, ChemCatChem. 7 (2015) 952–959. doi:10.1002/cctc.201402999.

[33] A.J. McCue, A. Guerrero-Ruiz, C. Ramirez-Barria, I. Rodríguez-Ramos, J.A. Anderson, Selective hydrogenation of mixed alkyne/alkene streams at elevated pressure over a palladium sulfide catalyst, J. Catal. 355 (2017) 40–52. doi:10.1016/j.jcat.2017.09.004.

[34] S.H. Pang, C.A. Schoenbaum, D.K. Schwartz, J. Will Medlin, Effects of thiol modifiers on the kinetics of furfural hydrogenation over Pd catalysts, ACS Catal. 4 (2014) 3123–3131. doi:10.1021/cs500598y.

[35] M.W. Tew, H. Emerich, J.A. van Bokhoven, Formation and Characterization of PdZn Alloy: A Very Selective Catalyst for Alkyne Semihydrogenation, J. Phys. Chem. C. 115 (2011) 8457–8465. doi:10.1021/jp1103164.

[36] N. Cherkasov, Y. Bai, E. Rebrov, Process Intensification of Alkynol Semihydrogenation in

a Tube Reactor Coated with a Pd/ZnO Catalyst, Catalysts. 7 (2017) 1–16. doi:10.3390/catal7120358.

[37] L.B. Okhlopkova, S. V. Cherepanova, I.P. Prosvirin, M.A. Kerzhentsev, Z.R. Ismagilov, Semi-hydrogenation of 2-methyl-3-butyn-2-ol on Pd-Zn nanoalloys prepared by polyol method: Effect of composition and heterogenizationNo Title, Appl. Catal. A. 549 (2018) 245–253. doi:10.1016/j.apcata.2017.10.005.

[38] N.C. Antonio J. Exposito, Yang Bai, Kirill Tchabanenko, Evgeny Rebrov, Process intensification of continuous flow imine hydrogenation in catalyst-coated tube reactors, Ind. Eng. Chem. (2019) submitted.

[39] N. Cherkasov, A. Exposito, Y. Bai, E. V Rebrov, Counting bubbles: precision process control of gas-liquid reactions in flow with an optical inline sensor, React. Chem. Eng. 4 (2019) 112–121. doi:10.1039/C8RE00186C.

[40] A.J. Exposito, Y. Bai, K. Tchabanenko, E. V. Rebrov, N. Cherkasov, Process Intensification of Continuous-Flow Imine Hydrogenation in Catalyst-Coated Tube Reactors, Ind. Eng. Chem. Res. 58 (2019) 4433–4442. doi:10.1021/acs.iecr.8b06058.

[41] Y. Bai, N. Cherkasov, S. Huband, D. Walker, R. Walton, E. Rebrov, Highly Selective Continuous Flow Hydrogenation of Cinnamaldehyde to Cinnamyl Alcohol in a Pt/SiO2 Coated Tube Reactor, Catalysts. 8 (2018) 1–18. doi:10.3390/catal8020058.

[42] N. Cherkasov, Y. Bai, A.J. Exposito, E. V. Rebrov, OpenFlowChem – a platform for quick, robust and flexible automation and self-optimisation of flow chemistry, React. Chem. Eng. 3 (2018) 769–780. doi:10.1039/C8RE00046H.

[43] https://sourceforge.net/projects/openflowchem/, (n.d.).

[44] J. Wolberg, Data analysis using the method of least squares, Springer-Verlag, Berlin, 2006.

[45] D. van Herk, P. Castaño, M. Makkee, J.A. Moulijn, M.T. Kreutzer, Catalyst testing in a

multiple-parallel, gas–liquid, powder-packed bed microreactor, Appl. Catal. A Gen. 365 (2009) 199–206. doi:10.1016/j.apcata.2009.06.010.

[46] N. Cherkasov, A.O. Ibhadon, E. V. Rebrov, Novel synthesis of thick wall coatings of titania supported Bi poisoned Pd catalysts and application in selective hydrogenation of acetylene alcohols in capillary microreactors, Lab Chip. 15 (2015) 1952–1960. doi:10.1039/C4LC01066C.

[47] U.K. Singh, M.A. Vannice, Kinetics of liquid-phase hydrogenation reactions over supported metal catalysts — a review, Appl. Catal. A Gen. 213 (2001) 1–24. doi:10.1016/S0926-860X(00)00885-1.

[48] J. Yue, G. Chen, Q. Yuan, L. Luo, Y. Gonthier, Hydrodynamics and mass transfer characteristics in gas–liquid flow through a rectangular microchannel, Chem. Eng. Sci. 62 (2007) 2096–2108. doi:10.1016/j.ces.2006.12.057.

[49] A.-K. Liedtke, F. Bornette, R. Philippe, C. de Bellefon, Gas–liquid–solid “slurry Taylor” flow: Experimental evaluation through the catalytic hydrogenation of 3-methyl-1-pentyn-3-ol, Chem. Eng. J. 227 (2013) 174–181. doi:10.1016/j.cej.2012.07.100.

[50] A. Günther, M. Jhunjhunwala, M. Thalmann, M.A. Schmidt, K.F. Jensen, Micromixing of Miscible Liquids in Segmented Gas - Liquid Flow, Langmuir. (2005) 1547–1555. http://pubs.acs.org/doi/abs/10.1021/la0482406 (accessed December 26, 2014).

[51] C.X. Zhao, A.P.J. Middelberg, Two-phase microfluidic flows, Chem. Eng. Sci. 66 (2011) 1394–1411. doi:10.1016/j.ces.2010.08.038.

[52] A. Günther, S.A. Khan, M. Thalmann, F. Trachel, K.F. Jensen, Transport and reaction in microscale segmented gas–liquid flow, Lab Chip. 4 (2004) 278–286. http://pubs.rsc.org/en/content/articlehtml/2004/lc/b403982c (accessed October 29, 2014).

[53] F. Trachsel, A. Günther, S. Khan, K.F. Jensen, Measurement of residence time distribution in microfluidic systems, Chem. Eng. Sci. 60 (2005) 5729–5737. doi:10.1016/j.ces.2005.04.039.

[54] T. Ouchi, C. Battilocchio, J.M. Hawkins, S. V. Ley, Process intensification for the continuous flow hydrogenation of ethyl nicotinate, Org. Process Res. Dev. 18 (2014) 1560–1566. doi:10.1021/op500208j.

[55] I.R. Baxendale, C. Hornung, S. V. Ley, J. De Mata Muñoz Molina, A. Wikström, Flow microwave technology and microreactors in synthesis, Aust. J. Chem. 66 (2013) 131–144. doi:10.1071/CH12365.

[56] H.S. Fogler, Elements of chemical reaction engineering, 1999. doi:10.1016/0009-2509(87)80130-6.

[57] N. Cherkasov, M. Al-Rawashdeh, A.O. Ibhadon, E. V Rebrov, Scale up study of capillary microreactors in solvent-free semihydrogenation of 2-methyl-3-butyn-2-ol, Catal. Today. 273 (2016) 205–212. doi:10.1016/j.cattod.2016.03.028.

[58] L.B. Okhlopkova, E. V. Matus, I.P. Prosvirin, M.A. Kerzhentsev, Z.R. Ismagilov, Selective hydrogenation of 2-methyl-3-butyn-2-ol catalyzed by embedded polymer-protected PdZn nanoparticles, J. Nanoparticle Res. 17 (2015) 1–15. doi:10.1007/s11051-015-3289-6.

[59] L.N. Protasova, E. V. Rebrov, K.L. Choy, S.Y. Pung, V. Engels, M. Cabaj, A.E.H. Wheatley, J.C. Schouten, ZnO based nanowires grown by chemical vapour deposition for selective hydrogenation of acetylene alcohols, Catal. Sci. Technol. 1 (2011) 768–77. doi:10.1039/c1cy00074h.

[60] N. Semagina, M. Grasemann, N. Xanthopoulos, A. Renken, L. Kiwi-Minsker, Structured catalyst of Pd/ZnO on sintered metal fibers for 2-methyl-3-butyn-2-ol selective hydrogenation, J. Catal. 251 (2007) 213–222. doi:10.1016/j.jcat.2007.06.028.

[61] M. Crespo-Quesada, M. Grasemann, N. Semagina, A. Renken, L. Kiwi-Minsker, Kinetics of the solvent-free hydrogenation of 2-methyl-3-butyn-2-ol over a structured Pd-based catalyst, Catal. Today. 147 (2009) 247–254. doi:10.1016/j.cattod.2008.09.035.

[62] E. V Rebrov, E.A. Klinger, A. Berenguer-Murcia, E.M. Sulman, J.C. Schouten, Selective hydrogenation of 2-methyl-3-butyne-2-ol in a wall-coated capillary microreactor with a

Pd25Zn75/TiO2 catalyst, Org. Process Res. Dev. 13 (2009) 991–998. http://pubs.acs.org/doi/abs/10.1021/op900085b (accessed May 20, 2013).

[63] M. Crespo-Quesada, A. Yarulin, M. Jin, Y. Xia, L. Kiwi-Minsker, Structure sensitivity of alkynol hydrogenation on shape- and size-controlled palladium nanocrystals: which sites are most active and selective?, J. Am. Chem. Soc. 133 (2011) 12787–94. doi:10.1021/ja204557m.

[64] Z. Wu, E. Calcio Gaudino, M. Manzoli, K. Martina, M. Drobot, U. Krtschil, G. Cravotto, Selective hydrogenation of alkynes over ppm-level Pd/boehmite/Al2O3beads in a continuous-flow reactor, Catal. Sci. Technol. 7 (2017) 4780–4791. doi:10.1039/c7cy01542a.

[65] D. Duca, L.F. Liotta, G. Deganello, Selective hydrogenation of phenylacetylene on pumice-supported palladium catalysts, J. Catal. 154 (1995) 69–79. http://www.sciencedirect.com/science/article/pii/S0021951785711487 (accessed February 5, 2014).

[66] S. Vernuccio, R. Goy, A. Meier, P. Rudolf von Rohr, J. Medlock, Kinetics and mass transfer of the hydrogenation of 2-methyl-3-butyn-2-ol in a structured Pd/ZnO/Al2O3 reactor, Chem. Eng. J. 316 (2017) 121–130. doi:10.1016/j.cej.2017.01.068.

[67] N. Cherkasov, A.O. Ibhadon, A. McCue, J.A. Anderson, S.K. Johnston, Palladium–bismuth intermetallic and surface-poisoned catalysts for the semi-hydrogenation of 2-methyl-3-butyn-2-ol, Appl. Catal. A Gen. 497 (2015) 22–30. doi:10.1016/j.apcata.2015.02.038.

[68] S. Kobayashi, M. Okumura, Y. Akatsuka, H. Miyamura, M. Ueno, H. Oyamada, Powerful Continuous-Flow Hydrogenation by using Poly(dimethyl)silane-Supported Palladium Catalysts, ChemCatChem. 7 (2015) 4025–4029. doi:10.1002/cctc.201500973.